Two-dimensional quiet time equilibrium for the inner plasma sheet protons and magnetic field

Chih-Ping Wang,[1] Larry R. Lyons,[1] Margaret W. Chen,[2] and Richard A. Wolf[3]

Received 24 August 2001; revised 6 June 2002; accepted 12 June 2002; published 26 December 2002.

[1] In order to study the quiet time proton flow and magnetic field in the inner plasma sheet resulting from electric and magnetic drifts, we incorporate a modified version of the Magnetospheric Specification Model with a modified Tsyganenko 96 magnetic field model to self-consistently simulate plasma sheet protons and magnetic fields with two-dimensional force balance maintained along the midnight meridian. The resulting equatorial proton flows and pressures agree very well with observations quantitatively. Because of this agreement, the simulated force-balanced magnetic field configuration should give more realistic plasma sheet magnetic field variations for quiet times than does the original T96 model. This 2-D self-consistent simulation reproduces the observed flows and pressures better than our previous 1-D self-consistent simulation. The improvement results from a more accurate modeling of the coupling between plasma and magnetic field in the 2-D self-consistent simulation. *INDEX TERMS:* 2700 Magnetospheric Physics; 2764 Magnetospheric Physics: Plasma sheet; 2753 Magnetospheric Physics: Numerical modeling; 2760 Magnetospheric Physics: Plasma convection. **Citation:** Wang, C.-P., L. R. Lyons, M. W. Chen, and R. A. Wolf, Two-dimensional quiet time equilibrium for the inner plasma sheet protons and magnetic field, *Geophys. Res. Lett.*, *29*(24), 2186, doi:10.1029/2001GL013984, 2002.

1. Introduction

[2] The flow in the Earth's plasma sheet is driven by solar wind energy that enters the magnetosphere and the energy is stored in the flowing plasma as increased plasma and in the tail lobes as increased magnetic pressure. Force balance is maintained between the plasma and magnetic field, ensuring steady plasma flow.

[3] The stored energy in the plasma and magnetic fields is the major energy source for geomagnetic disturbances such as substorms and storms. Therefore, simulating the plasma transport and energy storage in the plasma sheet is crucial to understanding the role of the plasma sheet in geomagnetic disturbances. Quiet time plasma sheet proton distributions have been modeled by *Spence and Kivelson* [1993]. Their results, together with the quiet time observations by *Wing and Newell* [1998], showed that magnetic drift as well as electric field drift is important for obtaining realistic particle distributions for quiet times. Modeling of plasma dynamics under an empirical magnetic field allows for the correct inclusion of magnetic and electric drift. However such an approach does not allow for the important self-consistent evolution of the magnetic field configuration with the plasma. Self-consistency requires that a technique be used to relax the empirical magnetic field model to provide plasma a force-free environment e.g., *Toffoletto et al.* [2001]. We previously modeled the quiet time plasma sheet proton distributions [*Wang et al.*, 2001] using a modified version of the Magnetospheric Specification Model (MSM) with the incorporation of a modified Tsyganenko 96 model. The modified T96 model, which combined the original Tsyganenko 96 model [*Tsyganenko*, 1995, 1996] with adjustable modification currents, provided a more flexible magnetic field than the original T96 model and was able to maintain a force balance with simulated plasma pressure at local midnight along the equatorial plane and to reduce the force imbalance in the z direction within the plasma sheet. Despite the lack of good force balance in the z direction, the previous simulation was able to reproduce quantitatively the general features of observed plasma distributions and flows within the inner plasma sheet.

[4] In the present study, we model plasma and magnetic field more self-consistently than in *Wang et al.* [2001] by incorporating a new set of modification currents into the T96 model to maintain force balance in 2 dimensions along the midnight meridian plane. This simulation results in 2-D self-consistent equilibrium for both protons and magnetic field, which reproduces more accurately the realistic quiet time plasma sheet than did previous less self-consistent simulations.

2. Simulation Description

[5] The transport of plasma in the plasma sheet is modeled by a modified version of the Magnetospheric Specification Model (MSM). The original MSM [*Freeman et al.*, 1993] calculates the bounce-averaged electric drift and magnetic drift of flux tubes filled with isotropic distributions of ions or electrons at a set of specified kinetic energies inside the closed field line region of the magnetosphere. Details about how the MSM simulates particle fluxes and distributions of plasma parameters are given by *Wang et al.* [2001]. Our main modification to the original MSM is to improve its boundary particle sources to be more realistic. The new boundary particle sources take into account particles originating from the distant tail and from the low latitude boundary layer and are built based on Geotail observations [*Paterson et al.*, 1998] and the results of the finite-tail-width-convection

[1]Department of Atmospheric Sciences, University of California, Los Angeles, California, USA.
[2]Space Science Applications Laboratory, The Aerospace Corporation, El Segundo, California, USA.
[3]Department of Physics and Astronomy, Rice University, Houston, Texas, USA.

0094-8276/02/2001GL013984

model [*Spence and Kivelson*, 1993]. This boundary condition, the electric field model, and the initial condition are described in *Wang et al.* [2001] and are the same as used in the present study.

[6] The original T96 model generates realistic large-scale magnetic field configurations, but its current density distributions have constraints that prevent it from being directly used to obtain a force-balanced field. We improve the flexibility of the T96 by adding a set of additional small-scale circular current loops [*Tsyganenko*, 1998]. The current loops, each obtained by spreading out an originally infinitely thin current loop over all space without violating the condition $\nabla \cdot \mathbf{B} = 0$, are used to represent a realistic spatial distribution of current density. The current of each current loop flows in a circle, and the current density spreads out with a characteristic thickness D. The direction and amplitude of the current are adjustable. The center of each circular loop is located at [$X_{GSM} = 0$, $Y_{GSM} = 0$, $Z_{GSM} = bR_E$]. Each loop is parallel to the equatorial plane, so the current flows within a cross section with an area $\propto D^2$ that is centered at $r = aR_E$ and $Z_{GSM} = bR_E$, where r is the radius of the loop. In this simulation, D is the same for each current loop and is assigned to be 0.23 R_E. The parameters (a, b) of each loop are assigned to a grid of a spacing 0.3 R_E equally in the radial and z direction within the region 2 $R_E < r < 30$ R_E and -6 $R_E < Z_{GSM} < 6$ R_E. The magnetic field generated by these current loops is then confined inside the T96 magnetopause by adding the magnetic field generated by the current loops' closure current flowing along the magnetopause [*Tsyganenko*, 1995] so the component of the magnetic field normal to the magnetopause is zero. We adjust the amplitude and direction of the additional current loops at each time step so that the magnetic force balances the plasma pressure gradient force in the x-and z directions in the plasma sheet along the midnight meridian and the lobe magnetic pressure is equal to the equatorial plasma pressure.

3. Simulation Results and Discussion

[7] A cross-polar-cap potential drop of 26 kV is used in this quiet time simulation, as in *Wang et al.* [2001]. We run the simulation until both the plasma and magnetic field in the plasma sheet reach a steady state, which represents 2-D equilibrium for the quiet time protons and magnetic fields.

[8] In this section we compare the results from our 2-D self-consistent simulation with observations and the results from a simulation in which the magnetic field is the original T96 field and is kept constant (later referred to as the "non-consistent" simulation) and from the simulation in which force balance is maintained only at the equatorial plane along the midnight meridian (results from *Wang et al.* [2001], which we call the "1-D self-consistent" simulation).

[9] The simulated total proton pressure at midnight along the equatorial plane from the 2-D self-consistent simulation is shown in Figure 1, together with the simulated pressures from the non-consistent simulation and the 1-D self-consistent simulation. The inner edge of the plasma sheet at midnight, which is the Earthward boundary of protons drifting from our model's tail boundary, is located at $X_{GSM} \sim -7$ R_E, and the simulated pressures along the midnight meridian are compared with the perpendicular proton pressure in the region -7 $R_E > X_{GSM} > -9$ R_E observed by AMPTE/CCE [*Lui and Hamilton*, 1992] (dashed-and-double-dotted curve shows a pressure profile from one near-midnight orbit). Even though there are observations from several satellites available beyond $X_{GSM} = -10$ R_E, we only plot the quiet time plasma sheet pressure from AMPTE/IRM [*Angelopoulos et al.*, 1993]. The reason for choosing the AMPTE/IRM data is that our simulations only model slow drift and the AMPTE/IRM data had been processed so the contribution from bursty bulk flows was not included. In addition, the same AMPTE/IRM data also provides measurements of flow velocity, number density, and electric field [*Angelopoulos et al.*, 1993, *Angelopoulos*, 1996]. As addressed in the discussion section, comparisons of these parameters from AMPTE/IRM with our simulation results allow us to investigate the realism of our simulated magnetic field. By comparing several different plasma parameters from the simulation with observations from just one data set, we avoid possible ambiguities in comparing different parameters obtained from different data sets. The AMPTE/IRM data plotted in Figure 1 are the mean values calculated using a 2×10 R_E^2 bin in the X_{GSM}-Y_{GSM} direction and the error bars are a fifth of the standard deviation about the mean. The simulated pressures beyond $X_{GSM} = -11$ R_E shown in Figure 1 have been averaged in the same manner as the measurements.

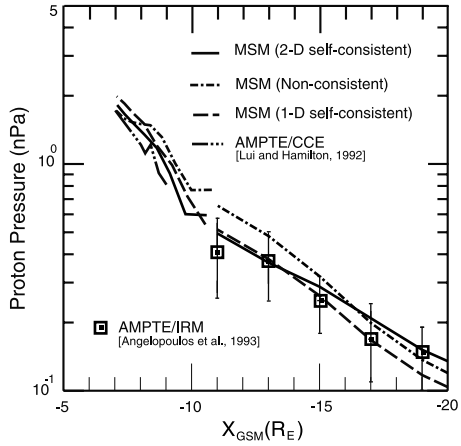

Figure 1. Quiet time steady state equatorial proton pressure (nPa) along the midnight meridian from the 2-D self-consistent simulation (solid curve), the non-consistent simulation (dashed and dotted curve), and the 1-D self-consistent simulation (dashed curve). Superimposed are the quiet time observations from AMPTE/CCE and from AMPTE/IRM. Note both the simulated pressures and the observation beyond $X_{GSM} = -11$ R_E are averaged over the region -10 $R_E < Y < 10$ R_E).

[10] In the region -7 $R_E > X_{GSM} > -9$ R_E, the simulated pressure from the 2-D self-consistent simulation is slightly more consistent with the AMPTE/CCE pressure than the non-consistent simulation or 1-D self-consistent simulation. Beyond $X_{GSM} = -11$ R_E, the 1-D self-consistent simulation brings the pressure to better agreement in the magnitude with the AMPTE/IRM pressure than the non-consistent simulation; however, the slopes in both profiles have sharper radial gradients than the AMPTE/IRM profile. With the 2-D self-consistent simulation, the radial profile becomes

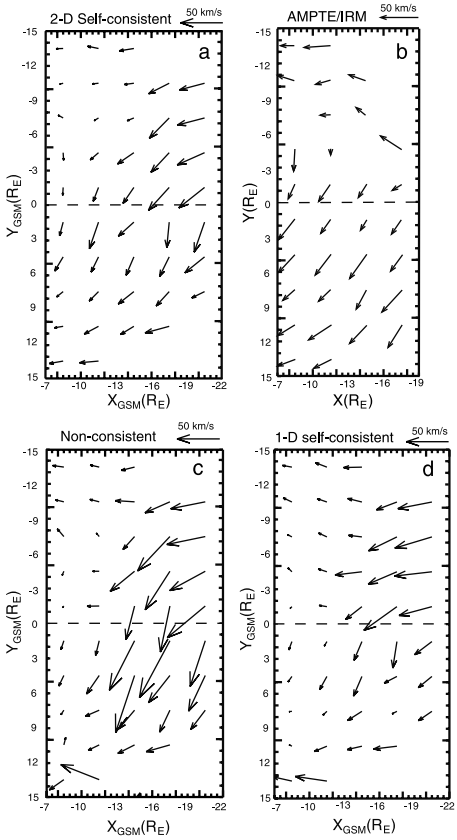

Figure 2. Quiet time proton flows in the equatorial plane from (a) the 2-D self-consistent simulation, (b) the observations by AMPTE/IRM [*Angelopoulos*, 1996], (c) the non-consistent simulation, and (d) the 1-D self-consistent simulation.

flatter and its radial gradient is closer to the AMPTE/IRM gradient. Thus the 2-D self-consistent simulation yields even better agreement with the observations than the 1-D self-consistent simulation. The comparison shows that the plasma transport under a force-balanced magnetic field results in a more realistic radial pressure gradient force, which is smaller than the force resulting from transport under a less consistent magnetic field. The decrease in radial pressure gradient occurs in conjunction with a decrease in the radial gradient of magnetic flux tube volume in the more consistent field as discussed later.

[11] The average velocity $\langle \mathbf{v} \rangle$ of protons in a time-independent magnetic field is

$$\langle \mathbf{v} \rangle = \frac{\mathbf{B} \times \nabla \Phi}{B^2} + \frac{\mathbf{B} \times \nabla p}{neB^2}, \qquad (1)$$

where n is number density and e is the electron charge. The first term on the right-hand side of (1) is the electric drift and the second term is the diamagnetic drift, which is the sum of magnetic drift and the magnetization effect. The proton flow within the equatorial plane from the 2-D self-consistent simulation is shown in Figure 2a. On the dawn side of the plasma sheet, the flow is dominated by Earthward electric drift. The duskward diamagnetic drift becomes as important as the electric drift around midnight and grows even stronger between $0 < Y_{GSM} < 6\ R_E$. Therefore the protons, which flow from the distant tail, are diverted toward dusk in the inner plasma sheet. The duskward drift gradually decreases as Y_{GSM} increases and the flow becomes Earthward again on the dusk side of the plasma sheet. The overall magnitude of our flow is lower than 50 km/s and the flow speeds around midnight are larger than those on the dawn and dusk sides. In general, this flow pattern and the flow velocities agree quite well with the quiet time flows from AMPTE/IRM [*Angelopoulos*, 1996], which are shown in Figure 2b. The proton flows from the non-consistent and 1-D self-consistent simulations are shown in Figures 2c and 2d, respectively. We can clearly see that the agreement with the AMPTE/IRM flow becomes better in both magnitude and direction of flow as the degree of self-consistency increases, especially around midnight where the 2-D force balance is maintained. The model flow speeds are consistently lower than the observations along the flanks; a disagreement that may be improved if force balance is extend to all local times.

[12] The equatorial magnetic field strength along the midnight meridian from the 2-D simulation is plotted in Figure 3 and compared with the original T96 magnetic field used in the non-consistent simulation and the modified T96 field from the 1-D self-consistent simulation. Both the simulated magnetic fields and the original T96 field show a decreasing strength with increasing distance from the Earth, but the radial gradient in the profile of the 2-D self-consistent magnetic field is quite different from those in the other two profiles. Beyond $X_{GSM} = -10\ R_E$, the 2-D self-consistent magnetic field has a flatter profile than the other two fields, which indicates that the magnetic flux tube volume in the 2-D self-consistent simulation decreases more slowly with decreasing distance from the Earth than in the other two simulations. With the assumptions of adiabatic convection and isotropic pitch angle distributions, this also

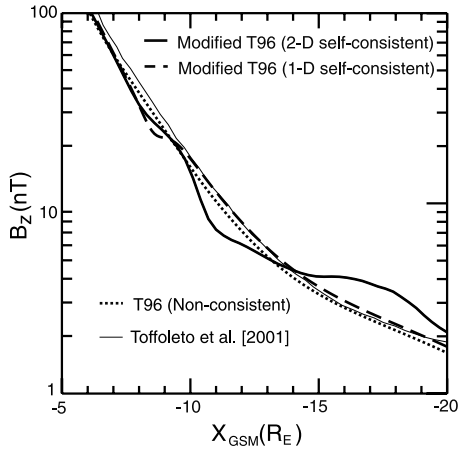

Figure 3. Equatorial magnetic field strength along the midnight meridian from the modified T96 model used in the 2-D self-consistent simulation (solid curve), field from the modified T96 model used in the 1-D self-consistent simulation (dashed curve), and field from the original T96 model used in the non-consistent simulation (dotted curve). The thin solid curve is the force-balanced magnetic field obtained by *Toffoletto et al.* [2001].

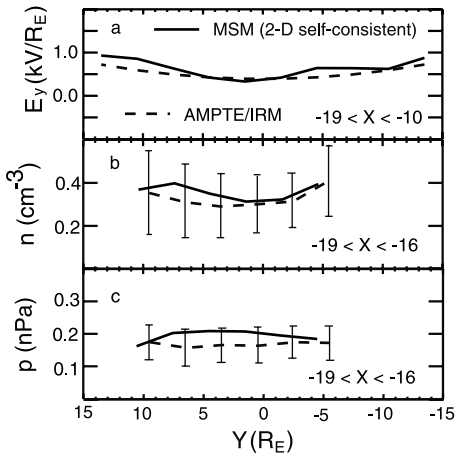

Figure 4. (a) The y component of the quiet time electric field across the tail averaged over the region $-10\ R_E > X_{GSM} > -19\ R_E$ from the 2-D self-consistent simulation (solid curve). Superimposed is a second order polynomial fit to the averaged E_y from AMPTE/IRM [*Angelopoulos et al.*, 1993] (dashed curve) over the same X_{GSM} range. (b) The number density and (c) the proton pressure across the tail averaged over the region $-16\ R_E > X_{GSM} > -19\ R_E$ from the 2-D self-consistent simulation (solid curve). Superimposed is the observed number density and pressure from AMPTE/IRM [*Angelopoulos*, 1996] (dashed curve) averaged over the same region.

implies that the particle energy density (pressure) increases more slowly with decreasing radial distance in the 2-D self-consistent simulation, which explains the improvement in the slope of the radial pressure profile from the 2-D self-consistent simulation shown in Figure 1. The force-balanced magnetic field profile obtained by relaxing the Tsyganenko 89 magnetic field for $Kp = 2$ using the *Hesse and Birn* [1993] relaxation technique [*Toffoletto et al.*, 2001] is also shown in Figure 3. This magnetic field was used by *Toffoletto et al.* [2001] as the initial condition for their simulations of the plasma sheet under enhanced convection. Their profile can be seen to resemble the original T96 field profile and to not show the flattening seen in our results. The difference with our results is likely because their relaxation technique tends to preserve the initial Tsyganenko magnetic field configuration and does not obtain the magnetic field by self-consistently modeling plasma and magnetic field.

[13] Restricted by satellites' orbits, it is difficult to obtain from observations a radial variation of the equatorial magnetic field strength along the midnight meridian that we can use to verify the magnetic field profile shown in Figure 3. We have shown good agreement of our simulated drift velocities and pressures with the AMPTE/IRM data. If our $\langle \mathbf{v} \rangle$, $\nabla\Phi$, n, and p all agree with observations, then equation (1) suggests that the magnetic field should also be realistic. Figure 4a shows the E_y from our electric field model and the E_y derived from the AMPTE/IRM data [*Angelopoulos et al.*, 1993] as a function of Y_{GSM}. The comparison shows that our electric field model represents the quiet time electric field realistically. Figure 4b shows that the calculated number density across the tail minimizes around midnight and becomes higher toward the dawn and dusk flanks; Figure 4c shows that the calculated proton pressure is relatively uniform across the tail with slightly higher pressure on the dusk side than the dawn side. Both profiles agree with the AMPTE/IRM data quite well, and they also agree qualitatively with the model results from *Spence and Kivelson* [1993] and the observations from *Wing and Newell* [1998]. Based on the above comparisons, we argue that we cannot get such good agreement with observations in all of the plasma parameters in equation (1) unless our magnetic field is also realistic. This quiet time magnetic field could be used as a realistic initial field condition for simulations of more disturbed magnetospheric conditions.

[14] **Acknowledgments.** We should like to thank N. A. Tsyganenko for his assistance in making modifications to the Tsyganenko 96 magnetic field model. This work has been supported at UCLA by NSF grant ATM-981698. The work by M. W. Chen has been supported by NSF grant NSF-ATM-9900981 and the Aerospace Technical Investment Program. The work by R. A. Wolf has been supported by NASA Sun-Earth-Connection Theory Program, grant NAG5-8136.

References

Angelopoulos, V., et al., Characteristics of ion flow in the quiet state of the inner plasma sheet, *Geophys. Res. Lett.*, *20*, 1711–1714, 1993.

Angelopoulos, V., The role of impulsive particle acceleration in magnetotail circulation, in *Proceedings of the Third International Conference on Substorms* (*ICS-3*), *Eur. Space Agency Spec. Publ.*, *ESA SP-389*, 17–22, 1996.

Freeman, J. W., R. A. Wolf, R. W. Spiro, and B. Hausman, B. Bales, R. Hilmer, A. Nagai, and R. Lambour, Magnetospheric specification model development code documentation, scientific description, and software documentation, contract F19628-90-K-0012, Rice Univ. for Air Force Geophy. Lab., Hanscom Air Force Base, Mass., July 1993.

Hesse, M., and J. Birn, Three dimensional magnetotail equilibria by numerical relaxation techniques, *J. Geophys. Res.*, *98*, 3973–3982, 1993.

Lui, A. T. Y., and D. C. Hamilton, Radial profiles of quiet time magnetospheric parameters, *J. Geophys. Res.*, *97*, 19,325–19,332, 1992.

Paterson, W. R., L. A. Frank, S. Kokubun, and T. Yamamoto, Geotail survey of ion flow in the plasma sheet: Observations between 10 and 50 R_E, *J. Geophys. Res.*, *193*, 11,811–11,825, 1998.

Spence, H. E., and M. G. Kivelson, Contributions of the low-latitude boundary layer to the finite width magnetotail convection model, *J. Geophys. Res.*, *98*, 15,487–15,496, 1993.

Toffoletto, F. R., R. W. Spiro, R. A. Wolf, M. Hesse, and J. Birn, Modeling inner magnetospheric electrodynamics, in *Space Weather*, *Geophysical Monograph Series Volume 125*, edited by P. Song, H. J. Singer, and G. L. Sisco, pp., 265–272, Am. Geophys. Un., Washington D.C., 2001.

Tsyganenko, N. A., Modeling the Earth's magnetospheric magnetic field confined within a realistic magnetopause, *J. Geophys. Res.*, *100*, 5599–5612, 1995.

Tsyganenko, N. A., Effects of the solar wind conditions on the global magnetospheric configuration as deduced from data-based field models, in *Proceedings of the ICS-3 Conference on Substorms*, *Eur. Space Agency Spec. Publ.*, *ESA SP-389*, 181–185, 1996.

Tsyganenko, N. A., Data-based models of the global geospace magnetic field: challenges and prospects of the ISTP Era, in *Geospace Mass and Energy Flow: Results From the International Solar-Terrestrial Physics Program*, edited by J. L. Horwitz, D. L. Gallagher, and W. K. Peterson, pp. 371–382, AGU, Washington, D.C., 1998.

Wing, S., and P. T. Newell, Central plasma sheet ion properties as inferred from ionospheric observations, *J. Geophys. Res.*, *103*, 6785–6800, 1998.

Wang, C.-P., L. R. Lyons, M. W. Chen, and R. A. Wolf, Modeling the quiet time inner plasma sheet protons, *J. Geophys. Res.*, *106*, 6161–6178, 2001.

M. W. Chen, Space Science Applications Laboratory, The Aerospace Corporation, P.O. Box 92957 M2-260, Los Angeles, CA 90009, USA. (Margaret.W.Chen@aero.org)

L. R. Lyons and C.-P. Wang, Department of Atmospheric Sciences, University of California, Los Angeles, 405 Hilgard Avenue, Los Angeles, CA 90095, USA. (larry@atmos.ucla.edu; cat@atmos.ucla.edu)

R. A. Wolf, Department of Physics and Astronomy, Rice University, Houston, TX 77251, USA. (wolf@alfven.rice.edu)